USGS Cooperative Agreement for Geodetic Monitoring Operations

Geodetic Monitoring Project Name: Continued Measurement of Fault Creep in the San Francisco Bay Area, and Continued Measurement of Creep and Long-Baseline Deformation in Southern and Northern California
Cooperative Agreement Number: **07HQAG0026**
Principal Investigator : Roger Bilham
Geodetic Project Web Site: http://cires.colorado.edu/~bilham/creepmeter.file/creepmeters.htm
Term covered by report: 2007-2010

1. Summary of project, focus of operations, and main accomplishments

The project has as its goal the monitoring of surface creep on California faults. Five creep-meters operate on the Hayward fault in the Bay Area, two at the extreme ends of the creeping zone in central California, and four in the Coachella valley in southern California. Maintenance is required because the instruments are occasionally vandalized, flooded, or damaged by lightning. The data are available on line with delays of a few minutes to a few hours. Two sites have no telemetry because of potential vandalism. Subsequent to acquisition the data are published on the web as cleaned ascii text files, processed to remove transmission glitches and/or mechanical resets needed to accomodate the cumulative offset of the surface fault.

The project also maintains the Long Baseline Tiltmeters at Long Valley. During the past three years we replaced many of its sensors with newly developed float sensors in a careful examination of anomalous behaviour of the north south arm of the water pipe. Electrical damage to the sensors in two of the vaults occurred in late 2009 and it was not possible to repair them with project funds. Their repair will occur inthe summer of 2010.

In that surface creep reduces the slip budget for future earthquakes a goal of the project is to quantify the reduction of this seismic slip potential. A corollary is to monitor potential accelerations in slip rate that reflect increased stressing of the faults that are creeping. During the past three years we have recorded accelerated creep signals on all the monitored faults following local earthquakes. The amplitudes of these are typically a few mm, but creep events on the Superstition Hills fault in 2008 and 2010 (>24 mm) are amongst the largest ever recorded.

Finally we conducted experiments to identify the source of apparent left lateral slip on surface faults. The source of these signals appears to be fault parallel strains induced by expansive clays. Fault normal expansion of the fault zone and compression of its flanks occurs with amplitudes of less than 0.1 mm during heavy rain, whereas fault parallel contraction between stream gulleys apparently exceeds 0.5 mm. The finding confirms that the shallow monuments we have used hitherto must be braced, and deepened.

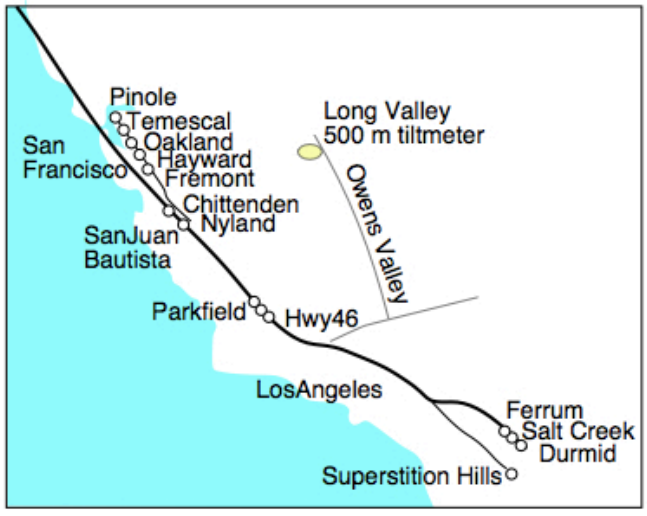

Fig. 1 Map showing instruments mentioned in the text. The Chittenden site has been terminated.

See section 3 (page 23) for map, numerical summary of locations, and numerical summary of observed creep rates

2. Describe in detail the work performed during the 3-year award period

The primary output from the project consists of web-based time series - lists of fault-slip vs time and on-line monthly, weekly and daily plots of slip. Should a local earthquake occur, or a large spontaneous creep event, numerous visitors check these web pages. Geologists use the data as a spring-board for field studies of triggered slip. Insar experts use the data to calibrate their models. Occasional publcations summarize the reduction of stress induced slip deficit on creeping faults

Much of the field-work in the past three years consists of maintaining this flow of data, replacing vandalized or flood damaged instruments, and replacing batteries. Approroximately eight visits to California have been undertaken each year for the past three years, half of which are funded by the project and half funded by the PI personally. Between these visits the data have been concatenated and published on the web.

The raw data are noise-limited by thermal effects and rainfall. Although each creep-meter is equipped with a temperature sensor, the direct compensation of thermal effects is rarely precise because the instrument and the ground respond to different frequencies and to spatially different applied temperatures. However, it is possible to halve the amplitude of the seasonal thermal signal (from ≈1 mm/yr to <0.5 mm amplitude) by low-pass filtering the temperature signal and subtracting an empirically determined fraction of the resulting time series from the observed displacement data. Although the resulting time series exhibits a smaller annual term, there is a danger that it can also add noise should the temperature sensor monitor signals to which the creep-meter does not respond linearly. Figure 2 shows five time series from the Hawyard fault that have been processed in this way to reveal surges in creep rate that are otherwise masked by seasonal signals.

Rainfall is typically a significant source of noise in creep data. It is suppressed in the Hayward fault creepmeters because the monuments consist of engineered steel tripods anchored deep in the muds adjoining the Hayward fault. These 2 inch thick steel shafts arranged in the form of a buried tripod resist moisture-induced expansion and contraction caused by dessication and saturation of surface muds. Because these seasonal effects amount to 2-3 mm in the shallow monuments of our other instruments, it is very desirable that we install deep monuments on the other creepmeters described in this report. Funds have never been made available to do this, but we shall propose to do this once more, in the next proposal.

In an attempt to quantify the source of precipitation-induced noise in shallow-anchored creepmeters we installed two fault-normal differential extensometers on the southern San Andreas fault. We hypothesised that fault gouge may be compressed by flank expansion during heavy rain. Others have proposed that a fault opens during slip as a result of asperities that must be over-ridden during fault slip. The results of this experiment are described in section **2B** of this report.

Finally, we note that we operate independent sensors and SUTRON and cell-telemetry (www.DataGarrison.com) on the Hayward fault. This has been perceived as a luxury by some critics. However the data from one has been used on occasion to patch interruptions to the other, and the cell telemetry we use provides graphic and numerical data on several time and resolution scales that can be accessed much more easily by the scientific community using the cell-based telemetry access page. While sympathetic to the needs of USGS Menlo Park, who use only the Sutron-based GOES satellite data (which have the important attribute of synchronized timing), it is important to realize that our cell-accessible telemetry is much more useful to the public, or even to USGS scientists in Caltech and other University groups in southern California. Since the telemetry costs only $180/per site per year we consider the abandonment of the redundant systems a false economy.

Section 2 is divided into subsections to address some of the detailed findings in the report. Section 2A relates creep measurements in the Bay Area of California. Section 2B discusses creep measurements south of San Juan Bautista to the Superstition Hills fault. Sections 2C, 2D and 2E discuss specific sites, and section 2F describes activities at

Mammoth Lakes. **Section 3** is the map requested in the template, and is accompanied by coordinates of the instruments. **Section 4** discusses data formats as requested in the template.

2A Hayward fault

The creep data are most easily assimilated as graphs, since the most important aspect of the creep data are departures from long term well-established creep rates that are readily identifiable in graphic form. Hence the first several figures consist of plots of data. However, the format of a 3 year report is not at all helpful for assimilating changes that occur over decades. In deference to the required USGS submission format we describe only the three year signal as indicated in the template provided, with scant reference to these decadal changes.

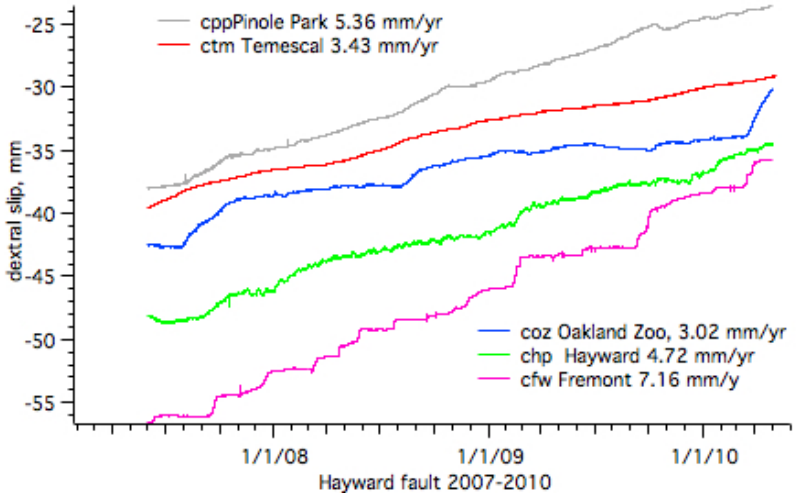

Figure 2 Summary of creep at five locations on the Hayward Fault. With exception of the first two the sites are 15 km apart and stacked from north to south. Thermoelastic contamination of the raw data have been suppressed for post-Nov 2007 data (see processing below). Creep events occur roughly 5 times each year at Fremont, and at 13-18 month intervals at Hayward and Oakland, but in southern Berkeley (Temescal Park) slip shows slow variations in rate superimposed in a slowing subsequent to an acceleration in slip in 2006.

With the exception of the data from Fremont, the data shown in Figure 2 are processed to suppress seasonal signals that reveal subtle changes in slip rate on the Hayward fault. Some investigators consider the seasonal thermal signal to be an important part of the measured data and use only the raw data in interpretations of the signficance of near-surface fault slip. The raw and processed data are shown in the individual site reports below, but in deferrence to the expressed needs of scientists in Menlo Park, only the raw data are made available as numerical time series on the web page where listings of these data may be obtained. The next five figures show raw and processed data from each of the five Hayward creep-meters so tht these data may be compared.

Highlights of Hayward data (fig1). Creep rates measured by creep-meters are typically 20% lower than those measured by alignment arrays at the same locations, indicating that not all the Hayward fault near surface strain is delivered to the fault trace as slip. Some is absorbed as near fault deformation, and some records the arc-tangent strain field of the fault locked at depth. The slip rate at Palisades Street has been steady for the past decade, while that at Oakland Zoo and Temescal Park show accelerations at the time of local microseismicity. At Pinole and Fremont we report an apparetn 10% increase in apparent slip rate although this is largely an effect of estimate the least squares trend from a short length of data. Eac of the five sites is discussed below.

cpp Pinole Park

Maintenance activities 2007-10, cpp Pinole: A 5V Sutron transmitter was installed in October 2007, before which the temperature trace was unreliable (straight line substituted in Fig.3). The creepmeter flooded early in 2007 and after operating underwater for a while that eventually damaged the A-D converters in the data logger. Shortly thereafter the LVDT was observed to be intermittently faulty and was replaced. Finally latency in the Verizon cell coverage was found to fluctuate, especially at night and weekends, resulting in delayed or lost data. The existing

Verizon link was replaced by an AT&T transmission link which due to the superior placement of repeaters in the northern Bay area reduced this problem. The temperature transducer was shifted in Sept. 2009 when a new LVDT was installed, and as a result the temperature correction applied to the bulk of the preceding data *adds* noise after this time. Further processing using a different empirical correction factor would improve the correction, but this improved correction is not attempted here. The point suffers from early morning mist which has required us to instal an additional solar panel to prevent the battery from dropping in winter conditions. An attractive wooden bar to inhibit bird excrement has been placed near the transmitting pole to encourage birds to perch away from the solar panels.

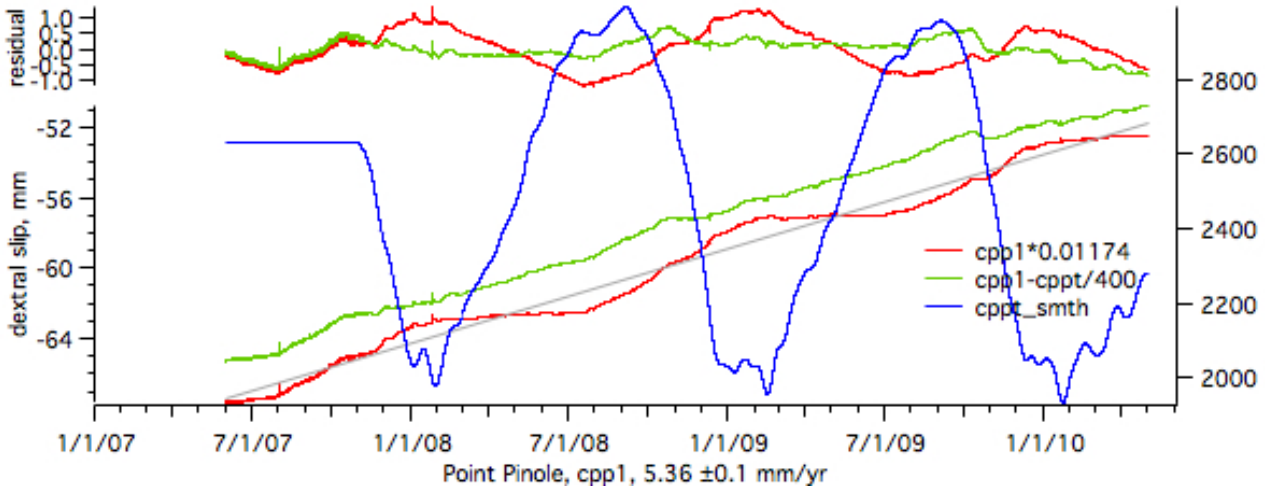

Figure 3 Raw and processed "cpp1" Pinole Park creep data. Red are raw and detrended data, with the indicated least-squares straight line fit removed. The subsurface temeprature has been low-pass filtered (blue trace with numerical count on right hand scale corresponding to annuual variation of about 15°C), divided by 400 and subtracted from raw displacement data, to produce the green data, in which the amplitude of the annual term is reduced to ±0.5 mm/yr. The smoothed temperature signals on the other creepmeter sites are similar to that shown for Pinole but are thus not shown in subsequent plots.

ctm**1 Temescal Park**

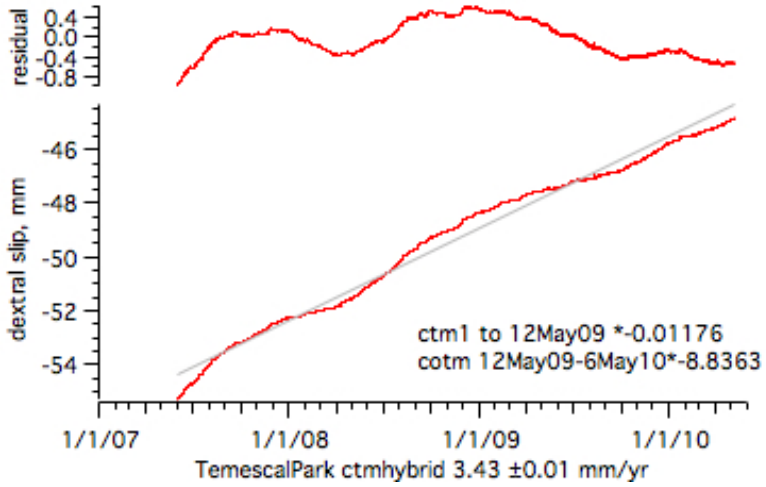

Figure 4 Creep and residual detrended creep from Temescal Park on the Hayward fault south of Berkeley. No suppression of thermal signal has been undertaken in these data

History of maintenance operations at Temescal Park: A 5V Sutron transmitter was installed in October 2007, and the ctm LVDT became inoperative in May 2009. The resulting data gap between its failure and replacement was filled with data from coTM, a second sensor at the site. In this hybrid plot the indicated calibrations are used for the separate segments of the data before and after May 2009. The detrended residual shows the slowing of the creep rate following a '06 creep event. The resulting least-squares linear fit (3.43 mm/yr) is applicable only to the three year time window presented above. The solar panels are placed on the roof of the Temescal Park machine shop where overhanging tree branches must be occasionally removed to keep the solar panels clear. The cell phone transmitter was found to suffer from extended latency due to a weak cell coverage

signal. This was remedied in late 2007 by with the addition of a YAGI antenna to increase its signal strength. In 2008 the black top was replaced above the creepmeter with no interruption to the record.

coz1 Oakland Zoo

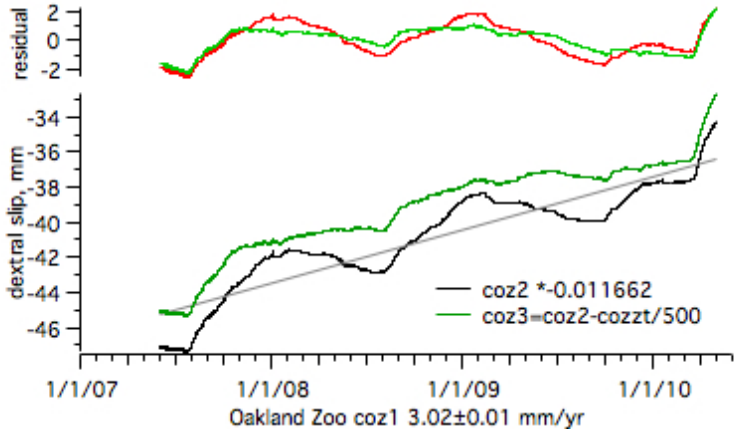

Fig.4. Raw (black) and thermally compensated (green) data from coz1 Oakland zoo for observed and detrended residual data. The creep rate here (3 mm/yr) is the lowest of all the Hayward fault sites we monitor but the signal is clearly interrupted by several month periods of accelerated creep (4-6 mm amplitude) that are often associated with microseismicity. The most recent started in April/May of 2010 as is most readily evident in the thermally adjusted data.

History of maintenance operations Oakland Zoo: A 5V Sutron transmitter was installed in October 2007. The temperature probe samples soil temperature near the transmitter box. Major landscaping by the zoo gardeners occurred in 2007, which improved security at the site but aggavated access to the sensors. The western vault is drained into the nearby creek and water runs continually through the creepmeter pipe in the rainy season. Additional data from a second sensor at this site are not shown but track the data well. The two sensors recorded 20µm and 30µm of slip at the time of passage of surface waves from the 4 April 2010 Baja earthuake. The site requires annual tree trimming to keep tree growth clear from the GOES antenna and the cell phone solar panel. Power is derived from AC from a outlet fuse box at the entrance to the park.

cpp1 Palisades Street, Hayward

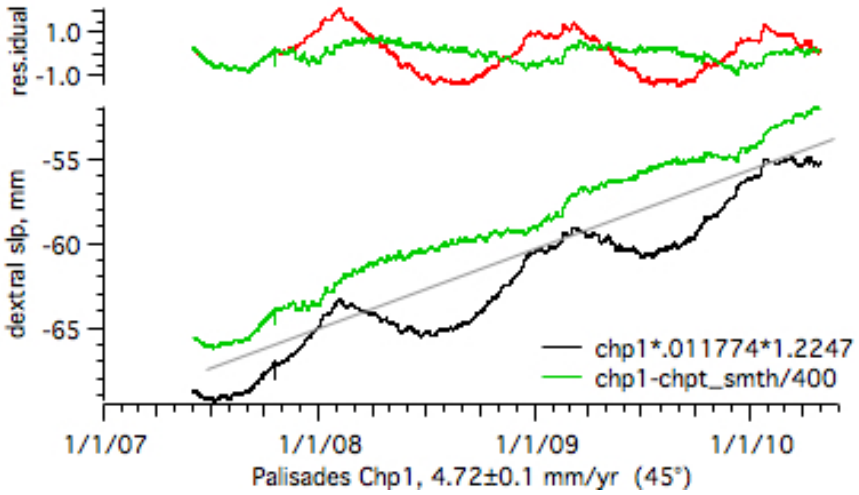

Fig 5 Creep data from cpp Palisades Street, Hayward. Black are raw data, and red are residual raw data with a least squares fit of 4.72 mm/yr removed. The green traces have had seasonal thermal signals reduced (as indicated) after October 2007 before which reliable temperature data are unavailable. The rate shown appears 22% higher than some previously published data from Palisades Street, which used a 30° obliquity correction instead of the actual 45°obliquity correction.

Summary of maintenance operations Palisades: A 5V Sutron transmitter was installed in October 2007. The temperature sensor lies in a tube in the shallow vault, and temperature changes here are large. Ants have infested the vault on occasion. The thermally corrected signal shows a suggestion that accelerated creep is aided by rainfall in the winter months. It was noted that an incorrect calibration signal had been applied to some earlier data which did not take into account the 45° obliquity of this site (all the other creepmeters are at 30 degrees and this site alone is at 45° since it is the reoccupation of one installed by Bob Nason 1960. The additional correction factor is x1.2247). In practice the site

misses some additional creep that is known to occur on a second fault trace some 50 m south of the creepmeter. The transmitter was flooded in 2009 but started operation again after water was drained from the internal antenna.

cfw1 Osgood Road, Fremont

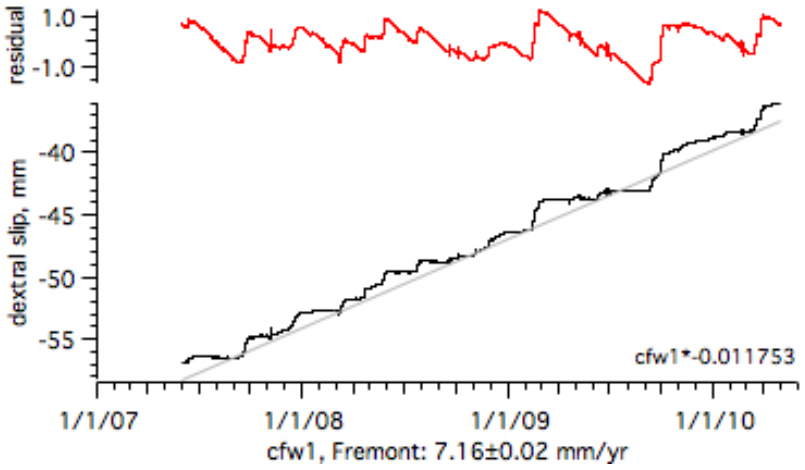

Fig. 6 2007-2010 data from Fremont on the Hayward fault is dominated by creep events.More than half of these creep events occur when the strain attains some stress level (a time predictable model) at which moment slip no more than 1 or 2 mm occurs. In general, the larger the creep event the longer the time to the next creep event. This creepmeter has the fastest creep rate of any operating on the Hayward fault.

Summary of maintenance operations Fremont: Extensive road works occurred here for most of the past three years as part of the construction of an interchange across Osgood Road. The protective fence was removed for much of this time and theft of the cell transmitter occurred. The new transmitter required a Yagi antenna to link reliably with the cell network. Additional subsurface wiring was installed to power the data logger from solar panels.

2B Southern California Creep meters

The next section of this report describes data from the instruments south of the Bay Area - thirteen in all**.** Three creep-meters are located on the southern San Andreas Fault at Durmid Hill and one on the Superstition Hills fault, and one each are located at the ends of the creeping zone in central California (Nyland at the north and at Highway 46 in the south). All of these instruments are installed with less than perfect monuments and would provide considerably imroved data quality were monuments similar to those installed on the Hayward Fault adopted.

Maintenance details south of the Hayward fault.

We first summarize maintenance and operational details of nine creepmeters and four fault-normal extensometers south of the San Francisco Bay area 2007-2010. All the Data Garrison transmitters were supplemented with additional cabling to provide solar power to the buried data loggers. The Chittenden site was abandoned despite initial successes, due to legal procrastination on the part of Union Pacific attorneys. Two Mexican border faults were instrumented following triggered slip after the Mw=7.2 ElMayor earthquake using NSF funding.

Chittenden, coCB The 130 m long steel Logan bridge across the San Andreas fault was instrumented with a 2 inch range LVDT. 12 cm of post 1942 creep has occurred at this site. See detailed report below on data processing and thermal signals.

Nyland Ranch, coNR. Invar rod at 45° to San Andreas fault replaced the original Bob Nason wire creepmeter. See summary of data processing below. The 30 mm range transducer was replaced with a larger range unit in 2009.

Parkfield, co46 This consists of a 12 m Invar rod at 30 degrees to San Andreas fault. See summary of data below. Data were accidentally lost due to a poor battery connection Jan-July 09, however according to the mechanical displacement measurements there was no creep during this time interval. A new battery clip was installed to prevent this problem from recurring.

Ferrum, coFE. A 10 m graphite rod is installed below the disused railroad at 30 degrees to San Andreas fault. Data are shown in Figures 9 and 10. The sensor battery was flooded in January 2010 which caused six days of data to be lost. The satellite transmitter was replaced with an elevated cell transmitter in July 2008 permitting telemetry costs to be halved.

Ferrum, FEXS A 3 m graphite-rod crossing the fault at 90 degrees was installed Jaunary 2010

Ferrum, FEFX 3 m graphite rod flank extensometer at 90 degrees installed Jaunary 2010

Salt Creek, coSC This consists of a 10 m stainless-steel wire at 45-55° to San Andreas fault. Data shown in Figures 9 and 10. An empirical correction is used to suppress themally induced errors at this site. A stable numerical correction requires the temperature probe to be placed 1 m into the steel pipe that crosses the fault.

Durmid, coDU A 6 m graphite rod is installed at 30° to the southernmost San Andreas Fault. Data are shown in Figures 9 and 10. The creepmeter has functioned normally in the past three years and is the closest to the IGPP strainmeter on Durmid Hill. Batteries were replaced at 6 month intervals and a minor offset occurred when a truck was driven illegally near one end in late February 2010. Data were gathered manually after creep events were transmitted from telemetered sites.

Durmid, DUXS A 3 m graphite rod crossing the fault at 90 degrees was installed Jaunary 2010.

Durmid, DUFX 3 m graphite rod flank extensometer at 90 degrees installed Jaunary 2010.

Superstition Hills , coSH **A** 6 m invar bar at 30° rosses the fault. See processing details below. The creep signal here is dominated by a large creep event sequence in November 2007, and a triggered slip event on 4 April 2008. Both events required subsequent mechanical adjustments to keep the sensors within range. An additional 3 inches was added to the invar rod in mid April 2010 to accomodate future slip.

Border Fault West, coBW **A** 6m graphite rod was installed at 30° across the westernmost triggered rupture near the Mexican border.

Border Fault East, coBE 6m graphite rod on east triggered rupture near Mexican border installed April 2010

We next highlight the results from the fault-normal experiments that were designed to identify the origin of rainfall-induced noise in the data. The fault normal sensors also provide the possibility of monitoring fautl-normal motion during creep events. Some authors have suggested that fault slip is ubiquitously accompanied by dilatation of the fault as a result of fault-zone roughness (Brune and Thatcher, 2003). The experiment we describe was intended to be a first attempt at monitoring this fault-normal displacement. We have learned that to monitor this reliably we would need to install at least two fault normal sensors to measure the strain tensor across the fault reliably.

2B1. Fault-Normal Experiment - fault zone dilatation ?

In a study to quantify the near-surface moisture effects on the fault zone we installed two pairs of fault normal extensometers designated XS, across the fault, and FX to monitor strain in the flanks of the fault. These instruments, if perfectly orthogonal to the fault, would be expected to measure a zero signal in response to dextral slip on a. In practice, misalignments from 90° result in small measured signals in the presence of dextral slip. We discuss these below.

The instruments were installed in Jan 2010 to monitor the effects of clay expansion in and near the fault zone in an attempt to identify the source of ubiquitous left-lateral episodes in the creepmeters following periods of heavy rain. These episodes of apparent left-lateral slip are recorded at Nyland Ranch (San Juan Bautista), south of Highway 46 (Parkfield) and at Durmid Hill. They are not recorded by the Superstition Hills creepmeter which is mounted on sandstone, nor are they recorded by the Hayward Fault instruments whose mounts are deep engineered structures.

The monuments for these instruments consisted of a bipod formed from slotted angle section (vertical) and 3/4 inch diameter threaded rod (at 50 degrees) driven to refusal and bolted at their top ends. The length varied from 1 m to 1.5 m depending on resistance of the ground. The tops of the rods terminated 30 cm below the ground surface, to provide a 30 cm deep path for the graphite extensometer length -standards within their PVC sheath. These were intended to anchor the extensometers in the surface zone where we anticipate most of our noise sources lie.

Apparent left lateral slip would be recorded if clays on the *flanks* of the fault expanded and squeezed the fault *closed* during precipitation events. Were this process operative its effects should be repeatable and recoverable since drying should reverse the process, and because indefinitely continued fault zone contraction is clearly not possible. We hypothesized initially that shear strain in the fault zone causes the fault to dilate (en echelon cracks are observed at the surface during triggered slip), and that the closing of these resulting en-echelon cracks provides the compliance needed for periodic fault-normal contraction. Creep events should slowly open the fault; rainfall should rapidly close the fault. Our experimental results have falsified this initial hypothesis.

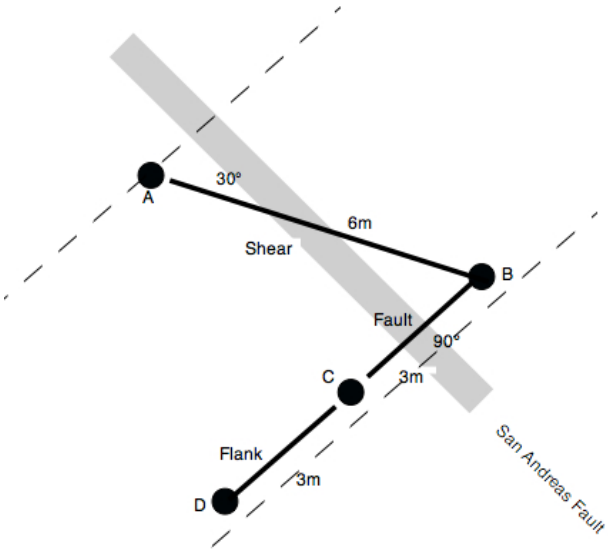

Fig 7 At Ferrum, creepmeter AB measures slip on the fault in a railroad cutting the base of which is indicated by dashed lines. Fault extensometer BC is sensitive to fault expansion, and flank extensometer CD is sensitive to flank contraction. All the extensometer rods consist of graphite maintained in tension with helical springs to prevent backlash in the LVDT sensors. The experiment revealed that fault-normal signals are small compared to fault parallel strains AC. At Ferrum clay expansion and unidirectional inward collapse of the sides of the rail-road cutting (illustrated by dashed lines) causes AC to contract.

A double extensometer normal to the fault, as illustrated in Figure 7, is sensitive to expansion or contraction of the fault gouge and of the materials in the rocks flanking the fault, but if installed normal to the fault cannot respond to dextral slip. On Durmid Hill both the fault gouge and flanking rocks are rich in clays whose dimensions swell in the presence of moisture. The fault-normal extensometers near coDU (Durmid) and coFE (Ferrum) were installed shortly before anticipated rain in the Coachella valley, and although rainfall was not measured locally we installed soil moisture sensors at 30 cm depth at each site to monitor subsurface moisture variations.

The three months of operation we report here includes triggered slip from the El Mayor earthquake. The polarity of the fault-normal signal accompanying this earthquake indicate that the extensometers were not installed precisely normal to the fault zone. One recorded opening and the other closing of the fault by amounts corresponding to misalignment by +12° and -4° respectively. More accurate alignment is difficult since the fault locally changes in strike by a few degrees over distances of tens of meters. It is now evident that three non-parallel components (a tensor array) would be needed to monitor true orthogonanl opening of the fault.

Notwithstanding the difficulty of monitoring fault normal displacements accompanying dextral slip, the extensometers, with one notable exception, provide an accurate measure of fault opening in response to moisture changes. The observed data show that, at both sites, the fault *widens* in response to increasing soil moisture, a process that is accompanied by *flank contraction.* The amplitudes of this effect (fractions of a mm) are small and result in a yet smaller *dextral* signal. This finding refutes our starting hypothesis that flank expansion follows rainfall.

The notable exception to measurement fidelity mentioned above was caused by flooding of the excavated and backfilled hole for anchor D in Figure xxx, which shifted 3.3 mm toward the fault 5 hours before the El Mayor earthquake. Points A, B, and C were stable during this 3.3 mm event. Subsequent inspection showed a pond had developed in the crater caused by its excavation, and we assume that the stiff clays were softened allowing abrupt stress relaxation of the bipod monument. Both flank extensometers extended ≈30μm (10^{-5} strain) during the triggered slip event 5 hours later.

The conclusion from the experiment is that contrary to speculation, fault-normal motions play a negligible role in generating the observed left-lateral signal that contaminates creep data in surface clays. Instead it would appear that

flank-parallel contraction must be responsible (ie contraction of the un-monitored, and tectonically uninteresting path AC). By far the largest flank contraction is observed at Ferrum, which lies at the base of a 4 m deep railroad cutting, and which hitherto we assumed would be the most stable of our installations. However, it is now obvious that the very nature of the cutting permits clays to expand into the excavated area and that when they do so they are driven by gravity, and are irreversible. ie the cutting incrementally closes at the time of heavy rain. It is not difficult to invoke a similar but smaller process occuring between the gulleys that cut across the fault at the coDU creepmeter.

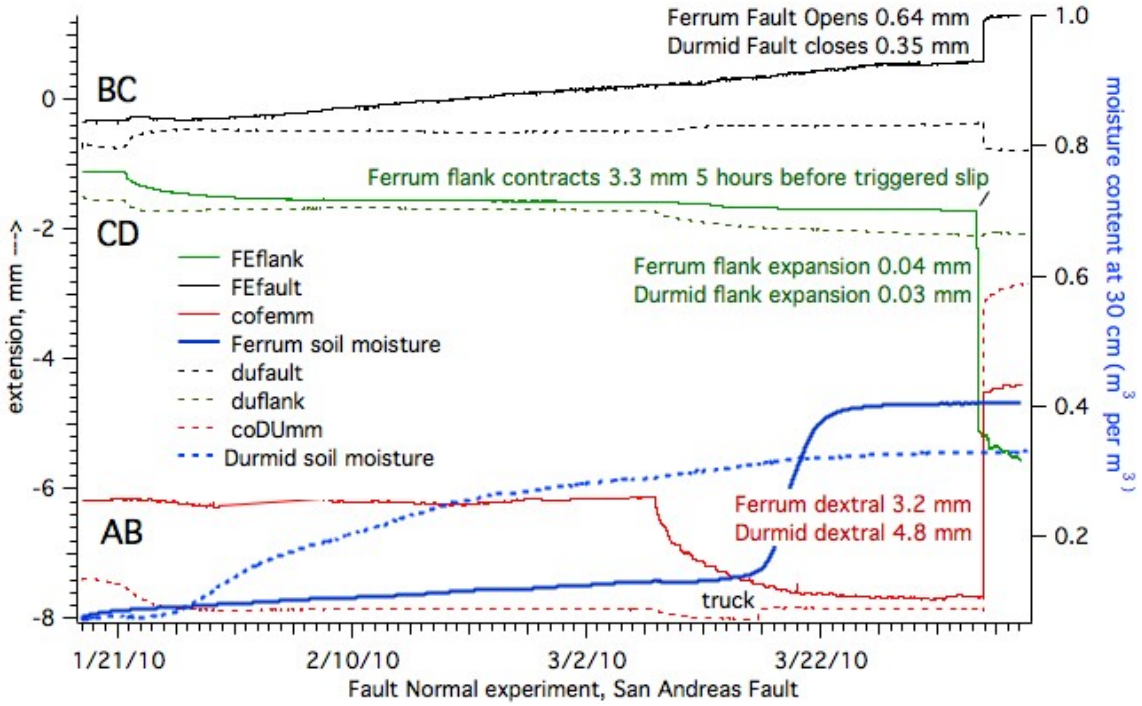

Fig 8. The above figure summarizes two months of data from the two fault normal extensometer pairs on Durmid Hill ((FE and DU) Solid lines are from Ferrum, and dashed lines from Durmid and the lettered pairs AB, BC, and CD correspond to the extensometer segments in the previous figure. Rain started 2 days after installation, and the blue lines indicate soil moisture content at 30 cm depth. On 7 March a large apparent left lateral signal at Ferrum AB accompanies torrential rain. The effect at Durmid is synchronous but a factor five smaller. An illegally driven truck almost crushed the Durmid AB instrument 17 March. Triggered slip produced minor expansion of the flanks of the fault (CD) and components of dextral slip were measured by the AB creepmeters and also by the BC fault normal extensometers, due to their not being aligned precisely at 90°to the fault.

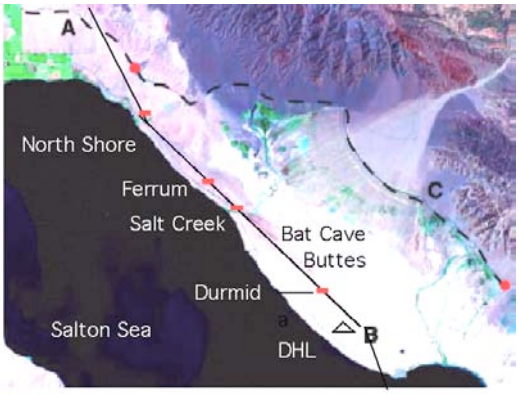

Figure 15 Location of creep meters on the southern San Andreas fault on Durmid Hill relative to the long baseline strain meter (DHL) operated by IGPP.
coFE Ferrum (33.4572°N , 115.8538°W) San Andreas Fault Durmid Hill,
coSC Salt Creek (33.44855 N 115.8437 W) San Andreas Fault Durmid Hill**,**
coDU Durmid Hill (33.4147 N 115.7985 W) San Andreas Fault Durmid Hill,.

2B2 Correcting the creep record for the effects of heavy rain?

Although the suppression of moisture-induced noise can only be achieved through the installation of improved anchoring arrangements, can moisture-induced errors in creep data on Durmid Hill be suppressed in existing data? We attempt this by eliminating all observed left-lateral data in the coFE and coDU data, and by replacing the resulting gaps in the data with offsets corresponding to the mean dextral slip rate observed during periods of drought. We justify manipulating the data in this way by invoking the finding that the clays are mobilized only during heavy rain and that the resulting downslope motion of muds into gullies etc are irreversible.

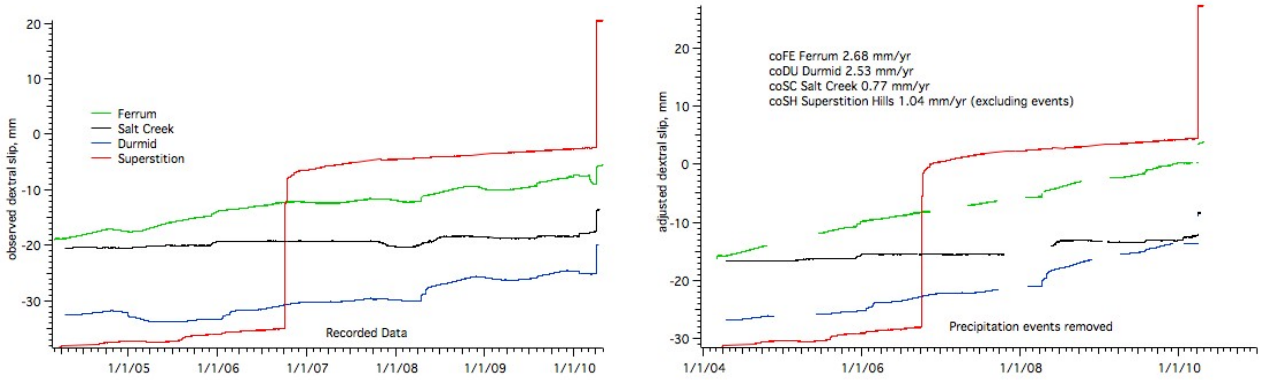

Figure 9 Upper left shows six years of observed data, and figure right shows the increased creep rate inferred for this time period when all sinistral slip data following heavy rain are removed and replaced by gaps corresponding to the mean slip rate observed at times of drought. Propagating creep events occurred on the southern San Andreas fault in 2006 and 2008. The prominent slip events on the Superstition Hills fault corresponds to a spontaneous 28 mm multiple creep event in late 2006, and 24 mm of triggered slip event at the time of the 4 April 2010 El Mayor Mw=7.2 earthquake. This creepmeter is unaffected by heavy rain because it is installed on bedrock.

In Figure 9 we demonstrate that the Ferrum and Durmid creep rates are almost doubled when left-lateral reversals are removed. The resulting inferred creep rate at Ferrum is 2.68 mm/yr and that at Durmid 2.53 mm/yr. The creep rate at the intervening Salt Creek site is less than 1 mm/yr. Although there is some uncertainty in the installation azimuth of the resuscitated Salt Creek Caltech) creepmeter, and hence the conversion of observed displacement to dextral slip slip, this cannot exceed 50%. Moreover the triggered slip amplitude at the Ferrum and Salt Creek differ by less than 10% for recent Baja earthquakes.

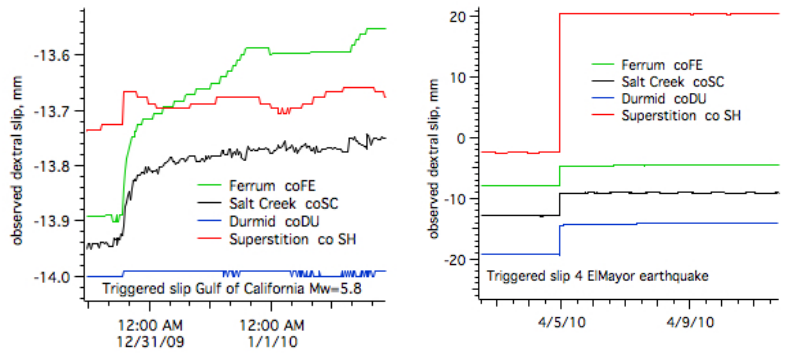

Fig. 10 Triggered slip in the Coachella Valley for Mw=5.8 (Gulf of California) and Mw=7.2 (ElMajor) earthquakes. Note the asymptotic decay of offset for the smaller earthquake but the incremental step function for the larger, closer earthquake. coFE and coSC register similar offsets despite their radically different designs (Ferrum uses a graphite rod, and Salt Creek a stainles steel wire held in tension by a beam balance)

2C. Logan Bridge, Chittenden, coCH

Logan bridge, Chittenden, crosses the San Andreas fault at 30° at the southern end of the 1906 rupture, south of the Loma Prieta earthquake, and north of the central California creeping zone at San Juan Bautista. Slip on the fault acts to drag the eastern abutment further from the western abutment. Despite the Mw=7.8 1906 and Mw=7.4 1989 earthquakes the slip deficit on the fault at this point exceeds 2m and some calculations show that it may exceed 4

m. Hence this segment of the San Andreas fault could slip in a 7.4<Mw<7.6 earthquake today. Two meters of fault slip would pull the western end of the Logan bridge from its new supporting abutment.

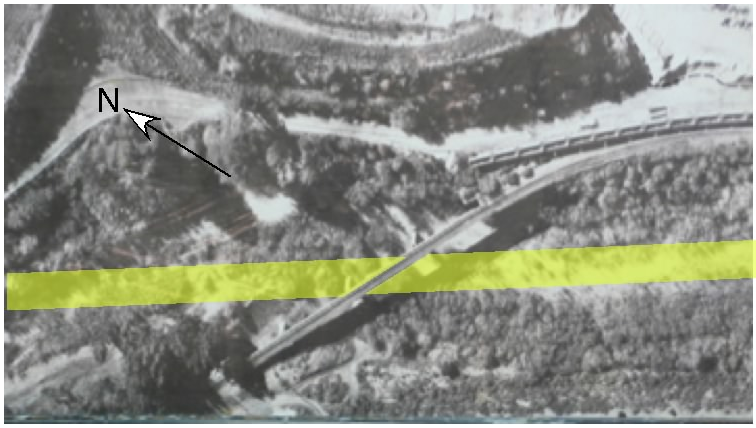

Figure 11 Areal view of Logan bridge crossing the Pajaro river at Chittenden, which here follows the San Andreas fault (yellow band). The western abutment lies at the lower left of the picture. The bridge is 130 m long.

In the 1906 San Francisco earthquake Logan bridge was dragged 1 m from its western abutment abutment. Bridge damage is described in the Larson report on the 1906 earthquake. After the earthquake, the bridge was repaired by supporting its western end on a temporary truss. In 1942 the bridge was rebuilt and straightened. At that time the railroad authority included two design features and two seismic safety elements to the structure to reduce seismic vulnerability. The first was the incorporation of roller bearing supports beneath the box girder on the westernmost piers and abutment. These accommodate both thermal expansion and approximately 30 cm of fault slip. The second design feature was the incorporation of a flat platform on the extended western abutment to permit a further 4 feet of drag by fault motion, beyond the rocker support path, to capture the deck before it separates from the western abutment.

Figure 12 LEFT: Lawson's view of the Logan bridge after repair in 1906. The photo shows a temporary vertical support filling the rail gap and a new trestle supporting the bridge itself. RIGHT: View (November 2008) of the roller-bearing n the western abutment nearing the end of its travel. The bearing was installed vertically in 1942 and the box girder has been dragged about 100 mm (1.4 mm/yr), 10 mm of which occurred since 1995. It is possible that 1/3 of this slip occurred in the Loma Prieta earthquake as triggered creep. The roller bearings have been pulled by (apparent) fault motion close to their point of unstable operation. Thermal expansion in summer rocks the arm a maximum 4 cm towards its central position.

The two safety features incorporated in 1942 consist of a seismometer on the penultimate western pier and a fail-safe link between the bridge and western abutment. The link consists of two weak conductors, which, if broken by eastward translation of the bridge, breaks a circuit to signals on the rail line, suitably arranged to arrest the approach of rail traffic from either direction. At the time of the Loma Prieta earthquake the link was not in working order,

the cables to the fail-safe link have been severed, and its cabling removed. This status has not been remedied since 1989. The status of the seismometer is unknown.

In January 1990, following the 1989 Loma Prieta earthquake we were given a copy of the construction plans of the bridge and permission from Southern Pacific to monitor bridge displacements. We installed a steel box containing a displacement sensor on the abutment and measured the changing distance between it and the free end of the bridge. The instrument recorded approximately 4 cm of post Loma Prieta creep on the San Andreas fault in the 5 months following the 1989 earthquake. We suspect that 2-4 cm of post-seismic slip may have occurred prior to our installing the monitoring device, and possibly as much as 1 cm subsequently. The instrument was maintained for 5 years but because it showed no significant additional slip, and since USGS funding was inadequate to maintain the recording device, its maintenance was discontinued after minor vandalism in 1995 (Figure13).

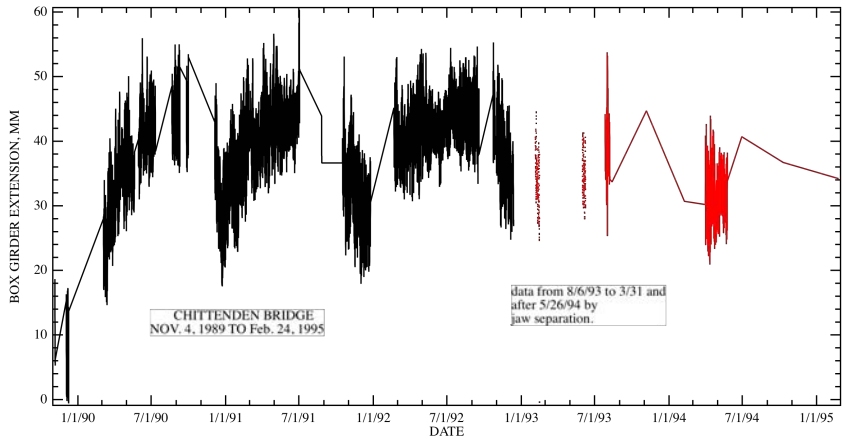

Figure 13 Data recorded by the 1990 recording system was discontinuous due to frequent power outages some of which were caused by vandalism. Approximately 4 cm of slip on the San Andreas fault occurred in the 5 months following the Loma Prieta earthquake. We suspect also that as much as 4 cm occurred before recording started and 1 cm may have occurred 1995-2009.

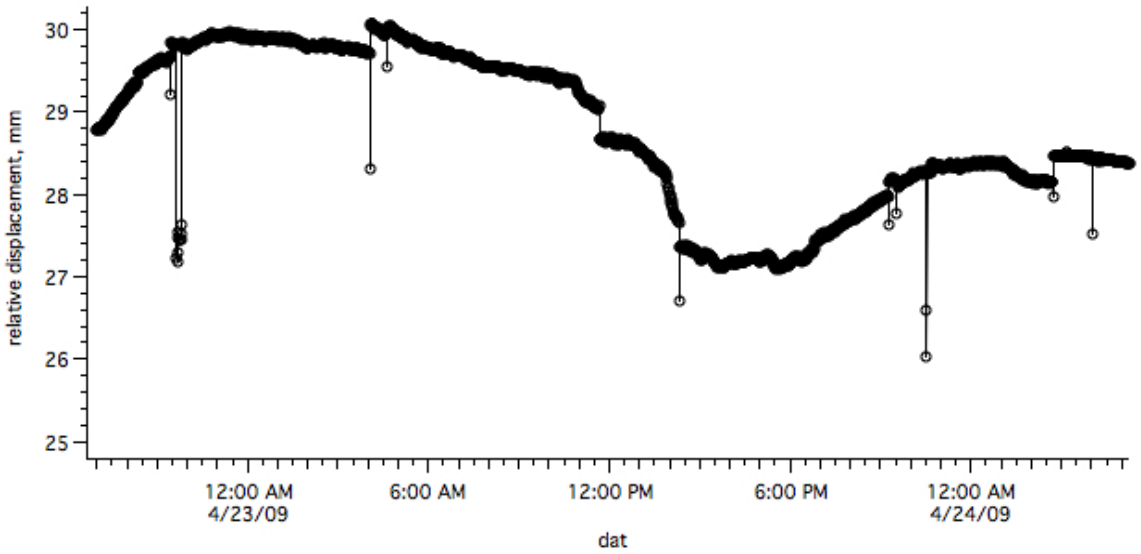

Figure 14 Data from Logan bridge showing transient changes of length caused by the passage of trains. Note four cases of offsets of ≈1 mm. Data samples (circled) are at 1 minute intervals

In April 2009, with renewed funding, we replaced the 1995 recording system with a low power autonomous recording system based on a 25-mm-range LVDT (Bilham et al., 2003) and an Onset data logger. We used a 1 minute sampling interval with 10 μm resolution. Loaded trains cause transient 1mm to 2 mm elastic changes in box-girder length, an effect which can be removed by electronic filtering. The passage of trains also introduces occasional static offsets of ≈1 mm, presumably as a result of overcoming frictional effects in the roller bearings (Figure 14). This effect is more problematical and imposes a limit to the accuracy in fault monitoring using the

bridge itself as a length standard. A significant challenge is to record a fault slip signal immune to the daily 15 mm thermal expansion of the bridge, and to the 40 mm annual variation in bridge length. The data recorded by the April 2009 test showed that thermal expansion effects could be reduced by 80% using data from a single temperature probe within the recording box, but that the long term thermal signal required a larger range displacement sensor. Subsequently in July 2009 we installed a 50 mm sensor.

The empirical correction of temperature is obtained in the 50 mm sensor by subtracting numerically 0.7 of the temperature change measured in degrees Celsius. This reduces the thermal noise to about 3 mm and has the advantage that it can be performed in real time as a linear subtraction. The mean apparent thermal expansion coefficient is thus 5.4×10^{-6}/°C, less than the coefficient for steel due to the location and filtered temperature time series measured by the temperature probe. We find, however, that the response of the bridge to temperature is not uniform since it is perturbed by direct sunlight which unevenly illuminates the box girder as shadows move across the hillside during the day. We subsequently installed several temperature probes to attempt a more complex empirical correction with the ultimate aim in reducing thermal noise to less than 1 mm. These have yet to be processed.

In mid-July, as the next step in providing a reliable signal to Southern Pacific, we tested cell phone data coverage. We found that coverage was poor below the level of the bridge box girder but excellent approximately 1.5 m above deck level. We considered cell phone telemetry would be satisfactory as long as the link could resist vandalism. Care was taken to hide surface cables from cursory inspection and to integrate the cabling with existing cables. The temperature corrected data (black trace) obtained from this pilot telemetry experiment (figure 6) demonstrate that correction to an accuracy of 1 mm appears possible.

On August 11th 2009 our sensor was erroneously removed by inspection engineers who were unware of our operational permit. Negotiations by supervisory engineers to reinstall the instrument were thwarted by an procrastination in the legal offices of Union Pacific, who indicated that they would revise and update our operational permit to cover future maintenance with the insertion of various waivers and legal exclusions. In May 2010, following 6 months of inaction and despite several written reminders from the PI, we requested that the sensor and transmitter be returned to us for use in other parts of the creep-meter program.

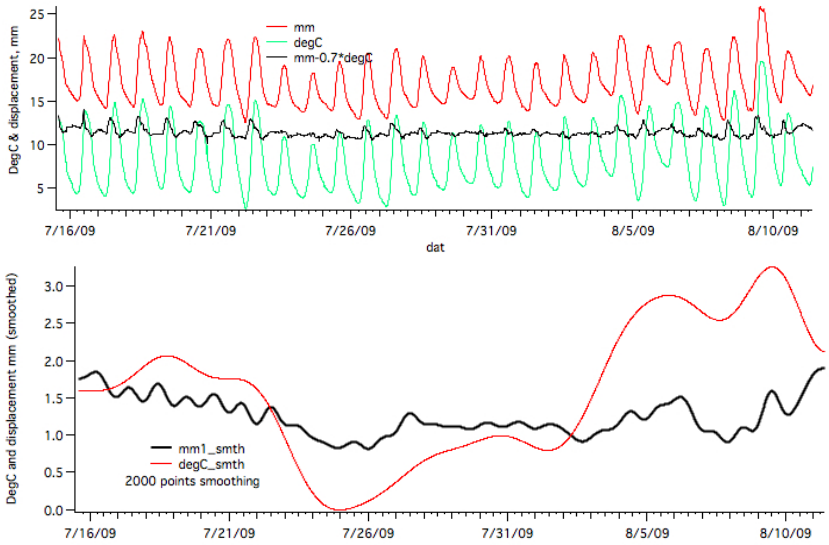

Figure 15 Data obtained from telemetry of thermal and displacement signal from west end of Logan Bridge. The black trace shows the temperature corrected displacement signal with residual thermal variations of less than 3 mm before smoothing, and less than 1.5 mm after smoothing. AT&T telemetry in July/August 2009 was limited to 15 minute samples. In an alert system based on the Iridium satellite the same low sample rate would be bypassed with a burst transmission of slip amount and duration to a list of email addresses and pager addresses.

2D. Nyland Ranch coNR

The creepmeter lies close to a fence that has been offset by more than 25 cm by creep at 9 mm/yr at the southernmost end of the 1906 rupture. Prof. Arthur Sylvestor's (Santa Barbara) nail-alignment array was destroyed in late 2008 when the road to Nyland Ranch was resurfaced. The high rate of slip on this instrument required its frequent mechanical resetting and a larger range sensor was installed 23 July 2009. The pre July calibration was 9.065 mm/volt. It is now 14.965 mm/volt. Rodents destroyed the signal cable in November 2009. The importance of this creepmeter is that it is located at the transition from creep to coseismic rupture, and slow earthquakes occur in this transition zone at depths of 4-6 km.

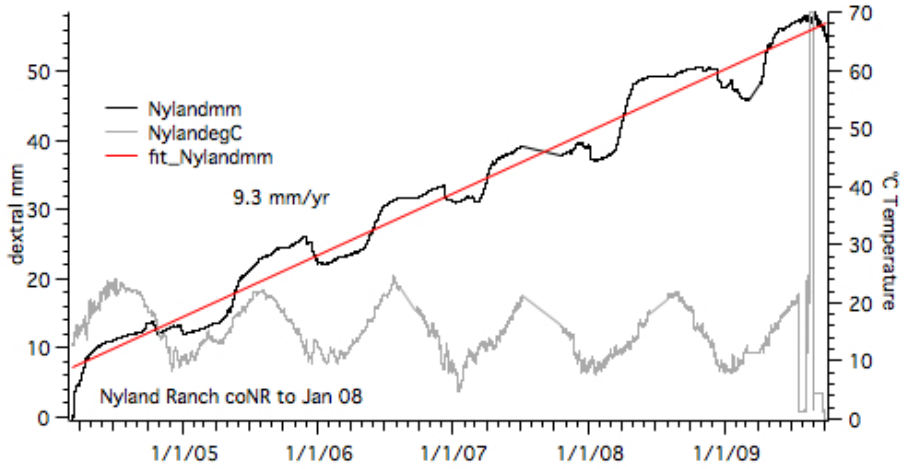

Fig. 16 Data from the creepmeter at Nyland Ranch suggests that at this location the left lateral reverals are indeed recovered during times of drought. The ground near the creepmeter is flat-lying and there are no gulleys to absorb clay expansion.

2E. Parkfield co46

The creepmeter lies close to a creepmeter operated by USGS. Its data suffer from left-lateral moisture induced events. The instrument is completely buried to avoid vandalism, however, it would be possible to instal a telemetery transmitter here, and we are considering doing this in 2010. The creep signal between times of rare rain consists to 1-2 mm amplitude creep events that in the past five years have resulted in cumulative slip of 20 mm . If we ignore the effects of rain-induced noise the slip rate is of the order of 2 mm/year here. Approximately 10 mm of afterslip occurred at the time of the Parkfield earthquake. A few months of data have been lost occasionally due to bad battery contacts, but according to our caliper measurements of the transducer, no cumulative slip on the fault has been lost during these data logging downtimes.

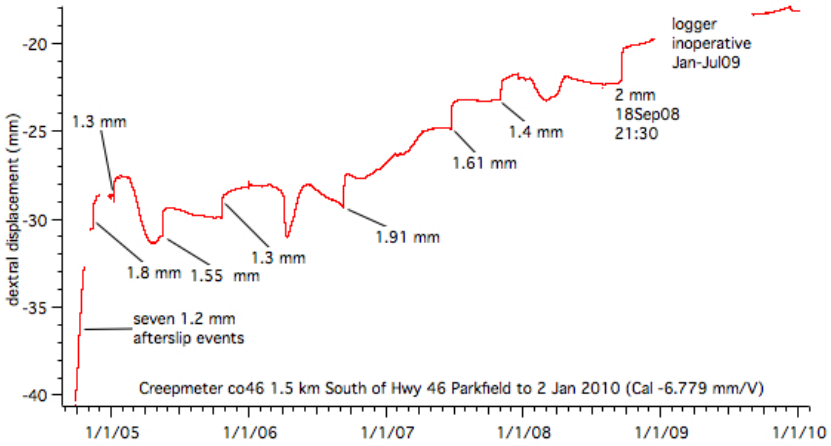

Fig 17. Data from co46, south of Hwy 46 at Parkfield. Gaps in the recorded data are followed by new contiguous data with the correct offset, as recorded by the transducer directly, and confirmed by micrometer readings.

2E, coSH Superstition Hills Fault.

In October 2006 the fault slipped 28 mm in a sequence of creep events, the first three of which are shown in Figure 18. Maximum slip rates were of the order of 0.5 mm/minute. See also Figure 9 and Wei et al 2009, and the moment release was equivalent to a Mw=4.7 earthquake.

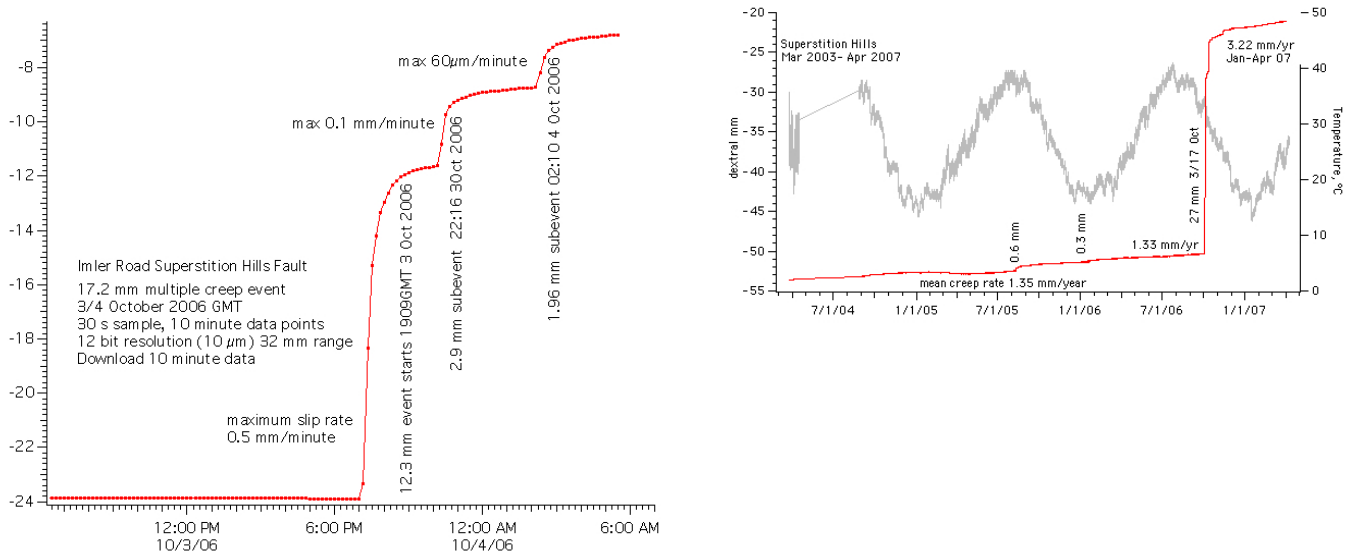

Figure 18 Slip on the Superstition Hills fault 2004-7 at approximately 1.3 mm/yr was interrupted in late 2006 by a spontaneous aseismic multiple slip event with a cumulative slip of 28 mm. The intervals between slip subevents with amplitudes of ≈2 mm increased from minutes to days terminating in a final slip event a month after the start of the sequence. The fault continued to slip at a ≈1 mm/yr rates until the ElMajor earthquake of 4 April 2010 when it slipped 24 mm in a single event with no afterslip. See Fig. 9.

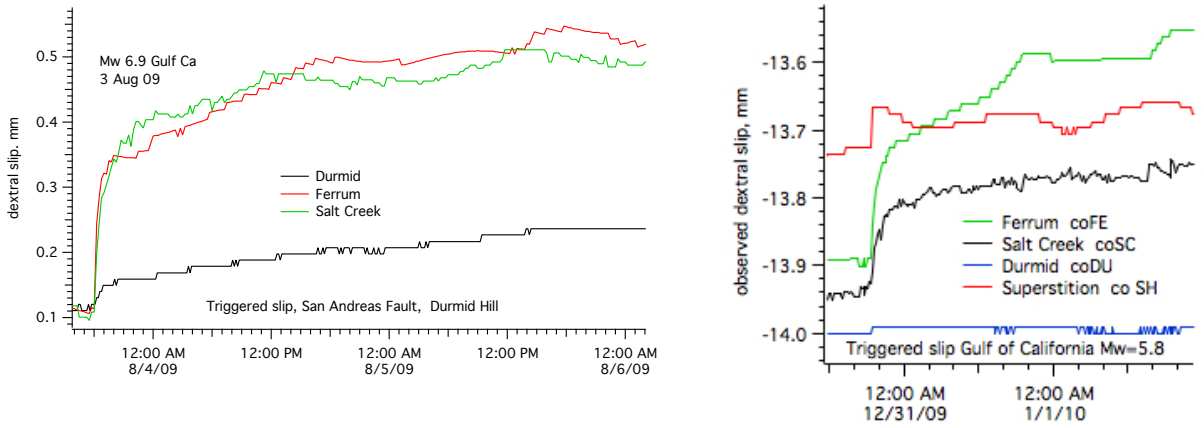

Figure 19 Triggered slip August 2009 and December 2009 shows an asymptotic continuation of slip following the causal earthquakes, whose time signatures differ strikingly from the abupt offset that accompanied the ElMajor 2010 earthquake.

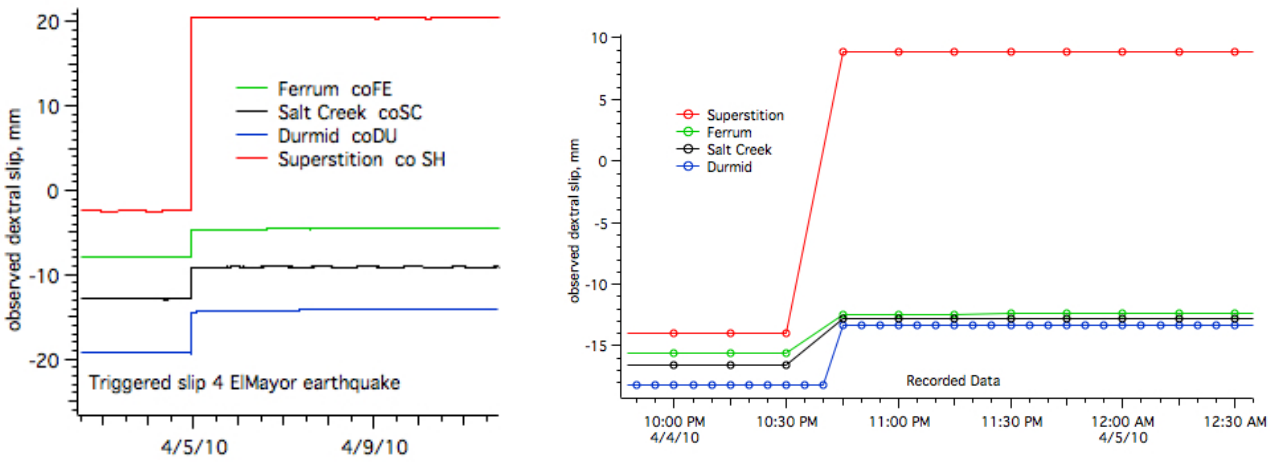

Figure 20 Two views of the triggered slip that accompanied the El Major earthquake, show it be of a distinctly different character from the spontaneous creep event sequences shown in Figure 18. Slip occurred between two contiguous 15 minute data samples. The very different geometries in the four creep-meters leads us to exclude the signal being an artifact of creepmeter construction. The coDU Durmid creepmeter was operating with a 5 minute sample interval, whereas the others record at 15 minute samples (to reduce telemetry costs).

2F Mammoth Lakes Long baseline Tiltmeters

The long-baseline tiltmeter in Long Valley is an essential component of the Long Valley alarm and evacuation scenario. Four M>6 earthquakes have occurred with 20 km of the instrument since 1980. The 15 km by 30 km Long Valley Caldera was formed during an eruption 760,000 years ago and is located 20 km south of Mono Lake along the east side of the Sierra Nevada in east-central California. When it erupted it scattered dust 2000 km downwind, and blasted out the eastern edge of the caldera. There have been multiple smaller eruptions since the caldera-forming eruption with the most recent occurring 250 years ago in Mono Lake at the north end of Mono-Inyo Craters volcanic chain.

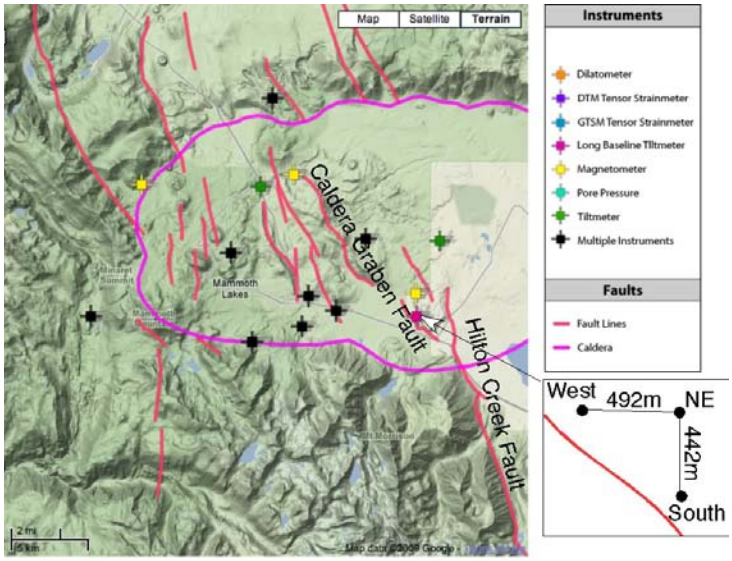

Figure 21. The 930 m long biaxial tiltmeter (inset geometry lower right) lies near the intersection of the Hilton Creek fault system and the caldera graben fault in the Long Valley caldera. Four Mw=6 earthquakes have occurred on this system since 1980. Strain changes accompanied a slow earthquake on the graben fault in 1992, the only reported instance of a normal fault linked to a slow earthquake.

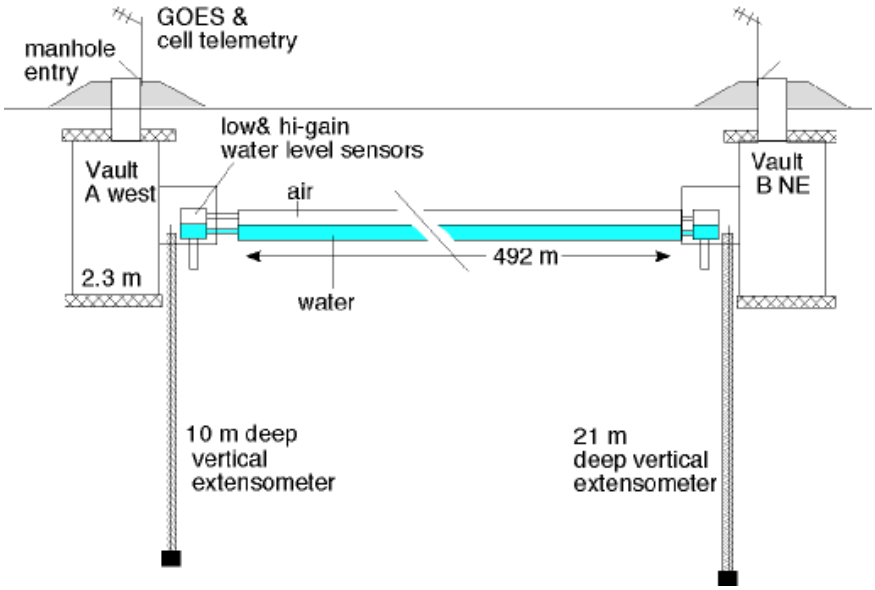

Fig. 22 Schematic section through the E/W arm of the long baseline tilt-meter in Long Valley. Data are transmitted by satellite links at each end of the water pipe. Altogether 22 channels of data from the instrument are recorded in Menlo Park. The heights of the water level (sensors with 6 mm range and 12 mm range), are referenced to the base of deep boreholes using a vertical extensometer consisting of a 6 mm diameter invar rod held in tension and monitored by an LVDT. Data from two of these extensometers are shown in Figure 30.

The tilt-meter consists of two orthogonal, horizontal buried pipes 492 m and 442 m long, which contain a continuous water surface that acts as a reference from which surface tilt is monitored by displacement transducers. Their transducers have a sensitivity of 0.1 μm, a range several cm and an inferred stability of 0.01 μm The original sensors used laser interferometers whose data were interrupted by local microearthquakes. Ripples on the surface caused the fringe pattern to be briefly lost, and its re-establishment led to an ambiguity in the fringe recovered. Recognising this shortcoming, these original sensors were replaced in 1993 with prototype float sensors designed to retain their datum through earthquakes and power cuts. From time to time we have improved the reliability and stability of these sensors using the tilt-meter water pipe as a test bed for innovation, since any number of sensors can be used independently to monitor the water level, and a measure of fidelity is obtained by the closeness with which new sensors track each other. Four generations of tilt sensor currently operate system, but only two of them are our most recent and lowest noise sensors. Using the technological advances tested at Long valley we have constructed three km-scale biaxial tiltmeters that monitor slow earthquakes in the Pacific northwest (see representative data Fig.2) , and a twelve-sensor, five component tilt-meter array in Pozzuoli, Italy.

In 2008, after almost a decade puzzling over an apparent malfunction of the north-south arm of the Long Valley Long Baseline Tilt meter, we finally identified its cause. The anomalous signal we observe is an apparent paradox: the north-south pipe records no semidiurnal tide at the south ends but records a semidiurnal tide at its north end. This appears to defy common sense until it is realized that the Earth's surface must be bending about a horizontal axis with a wavelength comparable to the length of the water pipe to produce the signal we observe.

Tests showed that the north-south tilt meter is functioning correctly. We ran a televiewer down the pipe to check for water continuity. We replaced all the sensors with newly calibrated sensors, and we undertook an in-situ intercalibration. The figure illustrates that the each pair of sensors in the tilt meter, though recording differences in high frequency oscillations of a wave advancing and reflecting from the ends of the pipe, records an identical incremental DC increase in height as a result of adding 7.5 litres at the center of the water pipe. We conclude that the sensors are not the problem, nor is the continuity of air or water in the horizontal north-south pipe. The signal must be in the Earth itself.

The floor of the Long Valley caldera is crossed by a fault that passes close to the south sensor of the tilt meter. A slow earthquake was recorded on the fault by the 11 sensors of the tilt meter in October 1998 suggesting that the fault normal stresses are low. The fault evidently acts as a vertical discontinuity that distorts the local strain tensor. As a result the caldera floor is flexing at tidal periods due to strain tilt coupling, which attenuates the O1 and M2 tides at the south end and leaves the tides at the north end unchanged. The south end of the tilt meter near the fault also responds to pressure loading. We have initiated a scientific report on this intriguing result, and are processing the 20 year record from the caldera for publication,

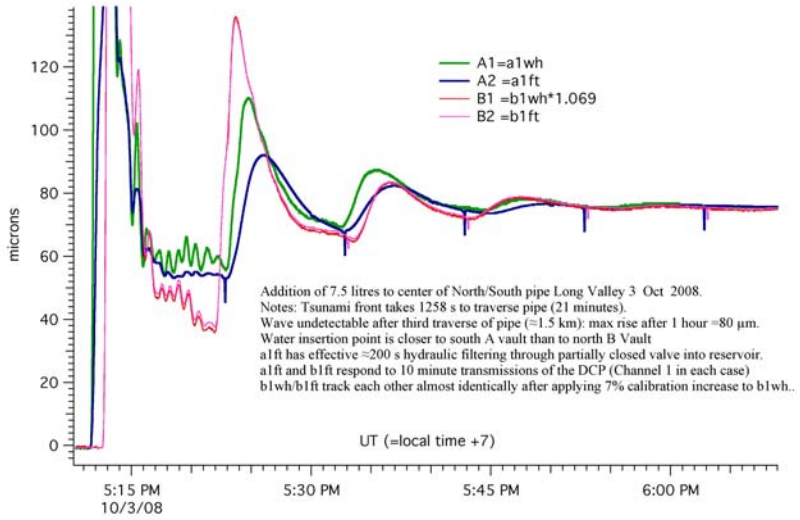

Figure 23 The response of the 452 m north arm of the Long Valley Tilt meter to the insertion of 7.5 litres of water near the center of the pipe. The water rises 79±0.5 µm on all four sensors and the oscillations of water-level are underdamped, with a fundamental period of ≈20 minutes.

In August 2008 we replaced five sensors in vaults A (south) and B (northeast) with new float sensors. With one exception the sensors retired were meniscus float sensors that had an undesireable propensity to during local earthquakes to undergo a several micron offset with a subsequent slow recovery. The exception to these retired units was the one remaining Chinese float sensor that was considered difficult to seal to be pressure-tight. The new floats consist of four chromium-plated copper balls within a PVC reservoir mounted on an adjustable pillar suspension. Since the pillar required the removal of the large aluminium base plates that had supported the previous sensors we also altered the mounting systems of the vertical extensometers.

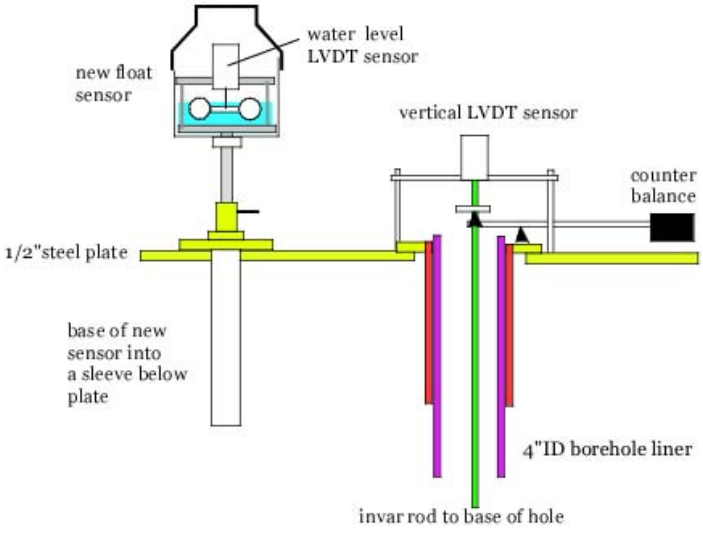

Figure 24 The figure illustrates schematically the new tilt sensor (left) whose pillar protrudes beneath the ½" horizontal steel plate in the support niche above the borehole extensometer in each vault. A screw collar permits the sensor to be raised or lowered over a range of 2.5 cm. An invar rod attached to the base of each borehole is held in tension by a beam balance (guided by flexure hinges shown symbolically as pivots in the figure). A detailed view of the flexure pivot arrangement is shown in Figure 5.

The tilt sensors that were replaced were a1wh & a1ft (north-south pipe south end), b1wh & b1ft (north-south pipe north end) and b2wh (east-west pipe east end above B vault borehole). The

south vertical sensor (A vault a1z1) was a ±0.25 inch range LVDT (±10V) that was recalibrated and remounted on two stainless-steel bolts. The northeast vertical sensor (±12 mm range LVDT) was replaced by a ±3 mm LVDT and was mounted similarly. The sensors that were not replaced or modified are b2ft (east-west pipe, east end, B vault wall), and c1wh & c1ft (east-west pipe west end), and c1z1 (the vertical extensometer in the west vault.

Table 1 Calibration and re-calibrations August 2008 (no changes to west C Vault)

Transducer	Code	µm/V	DCP Ch	a/d #	Logger #	Float gm	location
South A vault Transducers installed August 2008							
1556 (0.25")	a1ft	300	4	--		200.0	right
14499 (0.1")	a1wh	151	1	712324	1066364		left
10271 (0.25")	a1z1	622*	3	712439	1066364		back
temperature	onset	°C		1063297	1066364		Inside cover
pressure	onset	mbar		1011865	1066364		Inside vault
Northeast B Vault Transducers installed August 2008							
Temperature	onset	°C		768779	728203		inside cover
1557	b1wh	299	1	--		205.0	left
14474	b1ft	152	2	987136	728203	203.0	center
14547	b2wh	151	3	987133	728203	200.5	right high
15712	b1z1	141*	5	1083129	728203		back
--	b1wt	--	4	--			inside cover
Operating transducers removed &/or recalibrated							
9463	b2wh	144.72	3	987133			
15542	b1wh	133.82	1				
23884	b1ft	193.1	2		large bore unit returned to Boulder		
22335 (0.5")	b1z1	1263.03	5		½" range		
15712	a1wt	144.38	2	712434	reinstalled as b vault vertical b1z1		
J5182	a1ft	139.38	4	712439			
10269 (0.25")	c1z1	616.6	Vault C		Cal.9/12/08		

*In October/08 replaced with 129.84 µm/V -3 mm range sensor.
*142.04 µm/V in Onset scaling page

The new ±0.1"transducers were adjusted in the laboratory such that ±1.5 mm yields ±10Volts. They were then calibrated to 1% using a digital micrometer. Their calibrations are given in microns/volt.

In each vault there is now a large bore ±0.25" range transducer (low gain) and a ±0.1" range (high gain) transducer. The units are identified as follows

Low gain 6 mm range South-North a1ft-b1wh East -West **b2ft-c1ft**
High gain 3 mm range South-North a1wh-b1ft East-West b2wh-**c1wh**
c1wh is the last remaining meniscus sensor.

Figure 25. (left) Northeast (B vault) sensors in niche to east of access ladder. From left to right: b1wh (6 mm range) & b1ft (3 mm range) monitor the north

end of the north-south pipe, b2wh (3 mm range on galvanized column) monitors the east end of the 492 m long east-west water pipe right. Transparent lids and internal LEDs permit core alignments to be inspected.
Figure 23 (right) Sensor head of vertical extensometer. The PVC borehole lining that was flush with the ½" base plate at the base of the niche 20 years ago now protrudes 1 cm above the plate. The LVDT sensor is supported between the edge of niche wall and a stainless steel pillar (not shown) to the left. The bar to the right supports the counterbalance weight, a 6 inch long 2 inch diameter solid s/s bar. The frictionless mechanism of the flexure pivot holds the 3/8" diameter, 26 m long invar rod vertically, and styrofoam pellets downhole damp latitudinal vibrations of the invar rod. The LVDT core is mounted on a brass rod that is a pushfit into the stainless steel threaded collar protruding from the end of the invar rod.

Between 12-17 August 2008 Vault A (south) both meniscus float sensors were removed along with the aluminium table used to support them. New stainless steel sensors were bolted to the ½" thick base of the steel welded sensor box, and a door arrangement fastened to isolate the compartment from the seismometer vault. The new pillar supports required 9" tubes to be recessed into the base of the steel base plate. New air tubes and fittings were installed. In addition to the transmitted 12 bit DCP, the data are recorded by two local 12 bit data loggers. The DCP records ±10V, an Onset microstation 0-5V and a Hobo 0-2.5V. Despite their 5 Volt range the Onset microstations are presently arranged to record the full scale unipolar range of the transducer using a divide-by-two output at the transducer, and the 2.5V Hobo data loggers have an offset voltage and divider that permits them to record the full bipolar voltage output. The details from vault A are as follows

	USGS SUTRON DCP		ONSET microstation		Hobo
	sample	10min	10s/15 m		10 minutes
range	±10V	12 bit	0-5V	12 bit	0-2.5V 12 bit
a1wh	DCP1	0.15 mm/V	0.30 mm/V*		1.2 mm/V
a1ft	DCP2	0.3 mm/V	not recorded		
Thermistor	DCP3	approx.	not recorded		
Z	DCP4	0.6 mm/V	0.6 mm/V		
Pressure		mbar			
Temperature		°C			

* gain divided by two into 5V range, (i.e. 1.5 mm into 5 Volts fullscale) sampled every ten seconds and transmitted every 15 minutes . ** gain divided by 10 into 0-2.5V range

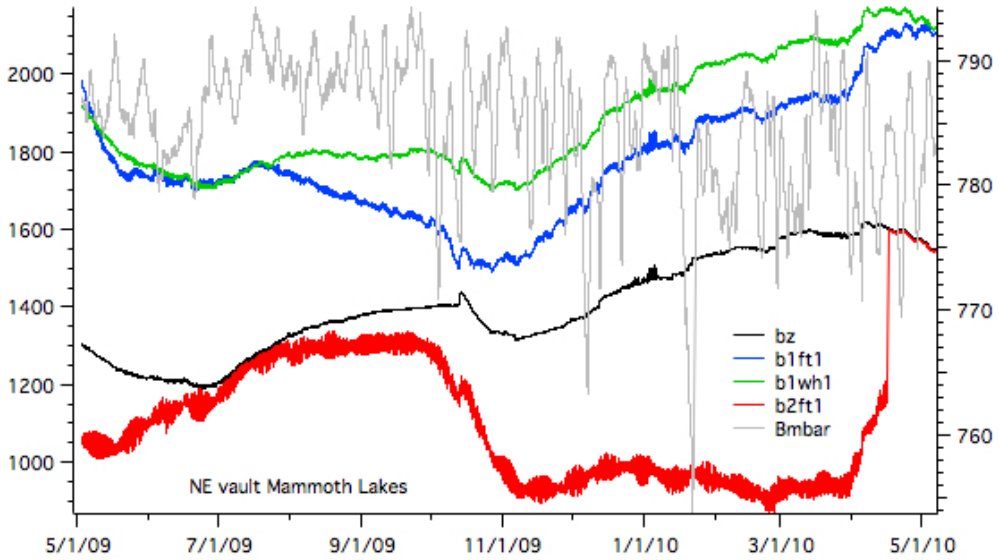

Figure 26 A year of data from the NE vault Mammoth with microns as the left hand axis and mb as the right hand axis. The data are corrected for vertical motion of the vault (bz). Note that significant low pressure fronts influence the water level at each end. b1 ft and b1wh are sensors on the north end of the north south pipe.

Summary of modifications A vault Dismantled Unit 15712 was 712434 to channel a1wh. Initial calibration was 6.926 V/mm. DataGarrison display factor 0.1394 Dismantled Unit J5182 was 712439 to channel a1ft Data garrison display factor was 0.138 with 0ffset .09 Initial calibration was 7.174 V/mm **a1ft** meniscus sensor abandoned and **a1wh** now a chromium float system. **a1wh** a/d 712434 is transducer 14494 with LVM110 calibrated ±1.5mm=±10Volts in parallel with Channel 1 of DCP. **a1wt** Thermistor into Channel 2 of dcp (not calibrated precisely) **a1z1** a/d 712439 vertical strain Transducer 10271 Type 250HPD Schaevitz into channel 3 of DCP (this was replaced a few weeks later by a 0.1" range sensor with a calibration constant of 129.84 µm/V).

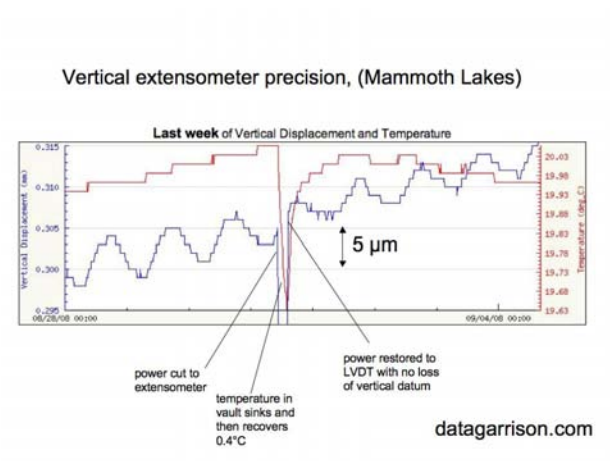

Northeast (B) vault. Both Aluminum support tables were removed along with three meniscus sensors. Three new chromium float sensors were installed (See Figure 20). The east sensor was mounted on a 3 inch galvanized iron pillar bolted to a pipe flange, which in turn was bolted to the base ½" steel plate. Regrettably the high gain sensor was misaligned on departure and a return visit was needed 12 August to correct this omission. A sample from the new B vault vertical extensometer sensor shows that it has a precision of 1 µm and is immune to short period thermal noise in the vault.

Figure 27 (left) Data from NE vault illustrating sensitivity of the new vertical extensometer sensor (see Figure 23) and its immunity to vault temperature during a recent power outage.

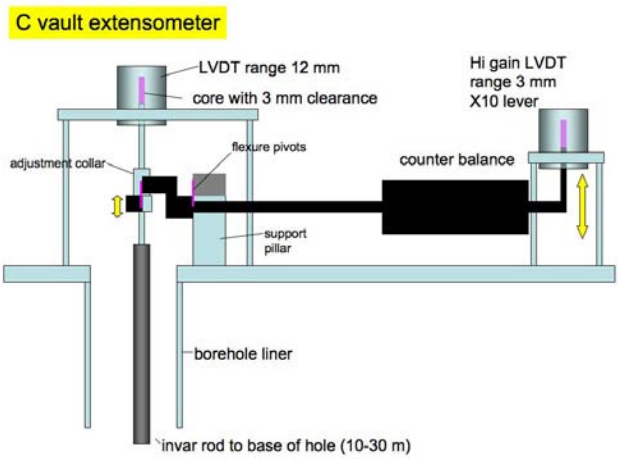

Fig. 28 Modified vertical extensometer in Vault C with low-gain and high- gain sensor. The sensor has high resolution (60 nm) but limited range (0.3mm). The extensometers in vaults A and B are not equipped with a high gain sensor but are otherwise mechanically identical.The mechanical gain of the vertical sensor is a factor of eight (not x10 as shown in figure 25). The transmitted scaling factor on the onset to April 09 is set at 56.597 µm/V.

West (C) vault . The vault was visited in August 2008 to verify its transmitted and recorded polarity. The invar rod rising relative to the base of the vault causes the voltage in the high gain sensor to fall. Hence voltage up means vault C up or positive strain change. Example data (fig 29) show that a temperature increase causes the vault datum to rise.

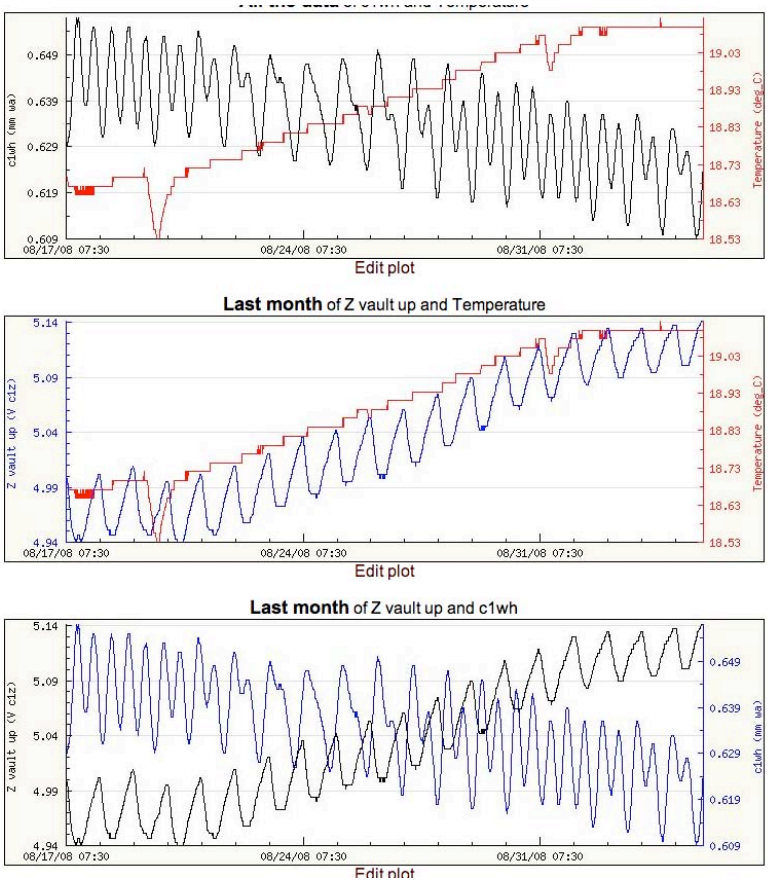

Figure 29 Two weeks of data from the west C vault illustrating thermal relationships and 40 nm sensitivity of the high gain vertical extensometer. The low gain sensor is transmitted via the DCP. and the high gain sensor via the Onset datagarrison link. Two power outages caused by work at the airport occur in the C vault during this time (temperature drops) but the backup batteries are able to maintain power to the system. The heating effects of the power supplies are evident from the temperature decay during the outages and its rise after power is recovered. The water level fall (50µm) in the time shown (which includes the east-west tilt component) is approximately thirty times larger than the vault level rise (≈1.7 µm).

A graduate student, Stephanie Higgins, expressed interest on working with the tiltmeter data and was supported on the grant to process the data from Mammoth Lakes for several months on 2008. She switched research topics shortly after starting but she was able to successfully reduce the vertical extensometer data since the start of the project.

These are shown in Figure 30.

A lightning surge damaged the A vault in 2009 and insufficient funds remained in the project to replace transducers and return the two water level sensors in the vault into operational status. New sensors are currently on order that will be installed in June 2010.

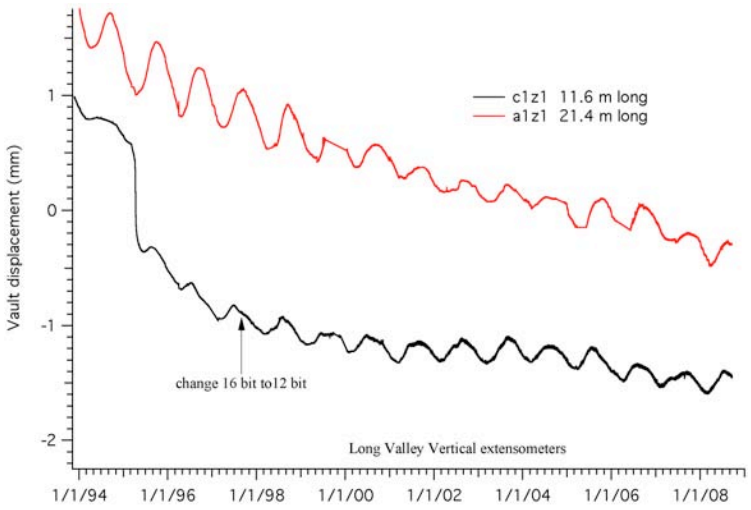

Fig. 30. Fourteen years of data from two of the vertical extensomers installed in 1993 to monitor vertical surface noise relative to ponts at depth. Vault settlement occurs currently at less than 0.5 mm/yr.

3. Map of Geodetic Stations showing telemetry

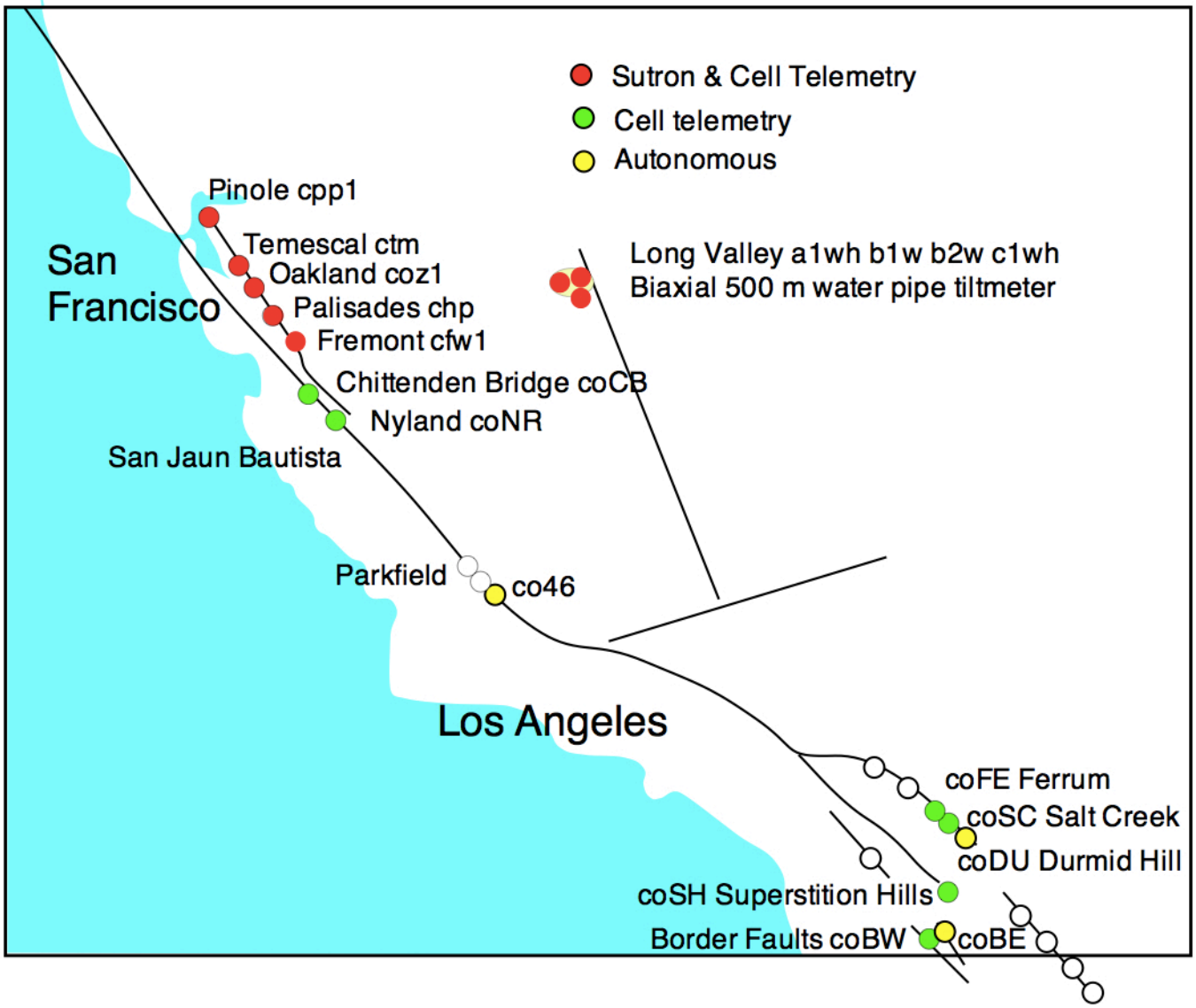

Figure 31 Map of creep-meters with site identifiers and symbols indicating the type of telemetry. Chittenden bridge was discontinued in 2009 due to legal slowness in renewing our permit to access Logan Bridge. Open circles are sites planned for creep monitoring by a RAPID NSF proposal, two of which are currently operating on the trans-border faults north of the Borrego fault in Mexico.

The sites near and south of the Mexico border are being installed collaboratively with CICESE as part of an initiative started by USGS in 2008.

Table 2. Summary of creep rates 2003/6-2007/10. Telemetered sites are shown in bold type. The least squares fits tend to underestimate true uncertainties especially for sites that undergo episodic slip. The mean creep rate on the Superstition Hills fault is dominated by two large creep events, the first of which in 2007 was spontaneous and consisted of a sequence of decaying creep events, and the most recent of which in 2010 responded to the coseismic strain field from the El Major earthquake as a single stp-like event.

Site	Location	2003_07 mm/yr	± mm/yr	2007_10 mm/yr	± mm/r	Change ±mm/r	Linear creep=L Episodic creep=E
cpp	**Pinole**	4.9	0.1	5.36	0.1	+0.5±0.14	L
ctm	**Temescal**	3.5	0.1	3.43	0.1	-0.1±0.14	E&L
coz	**Oakland Zoo**	3.1	0.1	3.02	0.1	-0.1±0.14	E&L
chp	**Hayward**	4.8	0.1	4.72	0.1	-0.1±0.14	L
cfw	**Fremont**	6.6	0.1	7.16	0.1	+0.6±0.14	E&L
coNR	**Nyland**	9.3	2	9.3	4-5	3	E&L
co46	S. Parkfield	3	1	2	1	-1.0±1.0	E
coFE	**Ferrum**	2.8	1	2.68	0.1	0.1±0.1	E&L
coSC	**Salt Creek**	1.5	0.3	0.8	0.05	1±1	E&L
coDU	Durmid	1	0.3	2.53	0.1	1.5±1	E&L
coSH	**Superstition Hills**	1.35	0.3	≈20		>19	E&L

Table 3 Site/monument information for Creep Meters

Site name	Site code	Creepmeter Type	**lat°N**	**long°E**	obliquity	monument
Pinole	**coPP**	30 m glass fiber	37.9892	237.645	30° H	tri-helix
Pinole	**cpp1**	30 m invar rod	37.9892	237.645	30° H	tri-helix
Temescal	**coTM**	30 m invar rod	37.8438	237.773	30°H	tri-helix
Temescal	**ctme**	30 m invar rod	37.8438	237.773	30°H	tri-helix
Oakland	**coOZ**	30 m invar rod	37.7527	237.85	30°H	tri-helix
Oakland	**coz1**	30 m graphite rod	37.7527	237.85	30°H	tri-helix
Palisades	**coHP**	30 m invar	37.6627	237.926	45°H	tri-helix
Palisades	**chp1**	30 m fiber	37.6627	237.926	45°H	tri-helix
Fremont	**coFW**	30 m invar	37.5323	338.048	30°H	tri-helix
Fremont	**coFW**	30 m graphite	37.5323	338.048	30°H	30m column
Nyland	**coNR**	8 m invar	36.855	238.454	45°SA	2 m column
Highway46	**co46**	14 m invar	35.7249	239.718	30°SA	2 m tripod
Ferrum	**coFE**	10 m graphite	33.45725	244.146	30°SA	2 m tripod
Ferrum*	**FEXS**	3 m graphite	33.45725	244.146	90°	1m bipod
Ferrum	**FEFX**	3 m graphite	33.45725	244.146	90°	1m bipod
Salt Creek	**coSC**	10 m steel	33.4485	244.156	45°SA	2 m column
Durmid	**coDU**	8 m graphite	33.4147	244.201	30°SA	2 m tripod
Durmid*	**DUXS**	3 m graphite	33.4147	244.201	90°	1m bipod
Durmid	**DUFX**	3 m graphite	33.4147	244.201	90°	1m bipod
Superstition	**coSH**	6 m invar	32.9301	244.299	30°SH	1 m tripod

* cross-fault/flank-normal extensometer pairs January 2010
"Tri-helix" signifies 10 m helical pile tripod anchors welded at fiducial measurement points.
"column" signifies vertical pile or drilled concrete column anchors.
"tripod" signifies steel rods driven to refusal and clamped and cemented at their fiducial points.
H signifies Hayward Fault , SA signifies San Andreas Fault, SH signifies Superstition Hills Fault
obliquity 45 degrees implies upgraded from 1960 vintage Caltech or Nason creepmeter

4. Data Management Practices:

For the operation of strainmeter and creepmeter instruments, the USGS requires that the network operator maintain the instrumentation at the site, and provide computer files of clean, processed data in geophysically meaningful units over the Web with a nominal latency of not more than six months.

Data for all of the sites except two are available with a latency of no more than three hours, and sometimes as short as three minutes. Usually no processing of the data is required since the displayed data are in mm and degrees C. Occasional malfunctions require data updates and these are posted on the web as ascii files.

Data from the two sites without telemetry (Durmid and CO46 near Parkfield) are collected every 6 months and concatenated into numerical time series on the web. These data are usually sent to John Langbein as an email attachment as soon as they have been acquired.

> *For creepmeter instruments, raw data must be available in near real time for internal use by the USGS to assist with hazards assessments (these data are currently provided via the GOES telemetry.)*

As explained above the data are available in real time. After significant events the data are processed and annotated in event pages on the web. eg. http://cires.colorado.edu/~bilham/LagunaSalada4April2010/Baja4April.html was available 4 hours after the earthquake. The data are usually compiled by the PI and sent out as attachments as an alert message. Note that the statement in parenthesis above is incorrect for the southern California CU Creep-meter array, since we do not have access to Sutron transmitters for the southern California sites.

> *For creepmeters, data must be archived with the Northern California Earthquake Data Center (NCEDC) in NCEDC standard format.*

The Hayward fault data are sent the NCEDC in SEED format from USGS Menlo Park using a script developed by Kathleen Hodgkinson in 2003. The following listings have been available on the NCEDC data base since that time.

SanFrancisco CFW 37.5300 -121.9600 FREMONT
SanFrancisco CHP 37.6600 -122.0800 PALISADES
SanFrancisco COZ 37.7500 -122.1500 OAKLAND ZOO
SanFrancisco CPP 37.6600 -122.0700 PINOLE PARK
SanFrancisco CTM 37.8400 -122.2300 TEMESCAL PARK
Mammoth Lakes a1ft
Mammoth Lakes a1wh
Mammoth Lakes a1wt
Mammoth Lakes a1z1
Mammoth Lakes b1ft
Mammoth Lakes b1wh
Mammoth Lakes b2ft
Mammoth Lakes b2wh
Mammoth Lakes b2ft
Mammoth Lakes b2z1
Mammoth Lakes c1ft
Mammoth Lakes c1wh
Mammoth Lakes c1wt
Mammoth Lakes c1z1

None, to my knowledge, use creep data in this SEED format. All strain, tilt and creep scientists access the data in more readily digestible formats.

I have not attempted to convert creep data for the southern California sites into SEED format hitherto because, like many of my colleagues, I do not know how to do this. The on-line streams require *embedded performance flags and frequent metadata*. Insufficient funds for programmer to undertake this formatting are available in the grant.

As explained at the geodesy meeting in Boulder April 2010, my strain and tilt colleagues and I consider the SEED format for long-period strain and creep data to be impenetrable and unnecessary. Almost certainly the upkeep of a SEED format output will double the salary line in the grant, and hence double the cost of the project. The doubling of the project cost to output the data in a format that strain-seismologists do not read seems to me a poor use of NEHRP funds, and is the stuff from which government whistle-blowing is made. Stated at its simplest I will include a three month salary line for a part time programmer in next year's grant proposal if NEHRP really wants the data in SEED format, despite my concernt that no one will ever access the resulting data in that format. Such money would be far better spent improving the anchors on the creepmeters, thereby improving the data quality, or in adding telemetry-overides to reduce data latency in the event of an earthquake.

References cited in the text

Behr. J., Bilham R. K. Breckenridge, P. Bodin and A. Sylvester, Afterslip on the San Andreas fault following the Loma Prieta earthquake. *USGS Professional Paper, 210-231,* August 1997

Bilham, R, N. Suszek and S. Pinkney, California Creepmeters, Seism. Res. Lett. 75(4), 481-492. August 2004

Bilham, R., and P. Bodin, Fault zone connectivity: slip rates on faults in the San Francisco Bay Area, California, *Science*, 258, 281-284, 1992.

Bodin, P., and R. Bilham, 3-D Geometry at Transform Plate Boundaries: Implications for seismic rupture, *Geophys. Res. Lett.* 21(23), 2523-2526, 1994

Brune J., and W. Thatcher, Strength and energetics of active fault zones, International Handbook of earthquake and engineering seismology Volume 81A 569-588.

Lawson, A., and H. F. Reid, The California earthquake of April 18 1906, Report of the State Earthquake investigation committee, Carnegie Institute, Washington, 1910

Wei, M., D.Sandwell,and Y Fialko, (2009), A silent Mw 4.7 slip event of October 2006 on the Superstition Hills fault, southern California, J. Geophys Res, 114,